International Journal of Pharmaceutics 383 (2010) 178–185

Contents lists available at ScienceDirect

International Journal of Pharmaceutics

journal homepage: www.elsevier.com/locate/ijpharm

Pharmaceutical Nanotechnology

In vivo and in vitro anti-cancer activities and enhanced cellular uptakes of EGF fragment decorated doxorubicin nano-aggregates

Shinyoung Park[a], Hyuk Sang Yoo[a,b,*]

[a] Department of Biomaterials Engineering, School of Bioscience and Bioengineering, Kangwon National University, Chuncheon 200-701, Republic of Korea
[b] Institute of Bioscience and Bioengineering, Kangwon National University, Republic of Korea

ARTICLE INFO

Article history:
Received 4 June 2009
Received in revised form 25 August 2009
Accepted 28 August 2009
Available online 2 September 2009

Keywords:
Nano-aggregates
Doxorubicin
EGF
Endocytosis

ABSTRACT

Doxorubicin nano-aggregate was prepared for the purpose of epidermal growth factor receptor targeted anti-cancer therapy. An epidermal growth factor fragment composed of 11 amino acids was conjugated to an amino terminal of bi-functional poly(ethylene glycol) and doxorubicin was subsequently conjugated to the other carboxyl terminal of the conjugate. A mixture of the conjugate, free doxorubicin, and triethylamine spontaneously formed nano-sized aggregates in aqueous phase, which was confirmed by transmission electron microscopy and dynamic light scattering. A549 cells incubated with doxorubicin nano-aggregates with the epidermal growth factor fragment showed increased endocytic uptakes of the aggregates compared to unmodified aggregates. Pre-blocking of the epidermal growth factor receptor on the cell significantly decreased a degree of the cellular uptakes. Cytotoxicity of the nano-aggregates was significantly increased when epidermal growth factor fragments were decorated on the surface of doxorubicin nano-aggregates, which was confirmed by a live/dead cell assay and a MTT-based cytotoxicity assay. When doxorubicin nano-aggregates were administered to model animals bearing human lung carcinoma, the epidermal growth factor fragment significantly strengthened in vivo anti-cancer effects of doxorubicin nano-aggregates compared to native doxorubicin or unmodified nano-aggregates. Thus, doxorubicin nano-aggregates decorated with an epidermal growth factor fragment is expected to be a potent anti-cancer agent aiming to tumor tissue over-expressing epidermal growth factor receptors.

1. Introduction

Doxorubicin nanoparticles have been extensively formulated for treatments of malignant tumors in aims to reduce undesirable side effects of conventional doxorubicin. Enhanced permeation and retention (EPR) effect mainly supports a passive targeting of the nanoparticulated anti-cancer agents (Allen, 2002; Blessing et al., 2001). Cancerous tissue has several distinctive vasculatures including defective formation of capillaries because substantial amount of blood should be supplied to fast-growing tissues. Nanoparticles with a size of several hundred nanometers can freely pass through the loose endothelial cell junctions in tumor tissues, while the passage is restricted by tight cell junctions in normal tissues. Therefore, numerous studies have been conducted to employ nanoparticulated anti-cancer drugs for potent cancer treatments. Doxorubicin was chemically conjugated to biodegradable polymer, poly(D,L-lactide-co-glycolide) [PLGA] to prepare doxorubicin nanoparticles (Brannon-Peppas and Blanchette, 2004; Brekken et al., 2000). Significant tumor regression was observed when the doxorubicin nanoparticle was intravenously administered to tumor-bearing animals. In other studies, doxorubicin and modified chitosan were formulated into doxorubicin nanoparticles by hydrophobic interactions between the anti-cancer drug and the hydrophobic polymer (Byrne et al., 2008; Ciardiello and Tortora, 2001). The doxorubicin nanoparticle showed comparable anti-cancer activity compared to native doxorubicin for 23 days. Folate was chemically conjugated to doxorubicin by a poly(ethylene glycol) [PEG] linker and formulated into nano-aggregates for tumor targeting (Freshney, 1994). In the study, folate-decorated doxorubicin nanoparticulates were efficiently endocytosed by cancer cells and showed enhanced cytotoxicities compared to native doxorubicin. Growth factors were also immobilized on nanoparticulated anti-cancer drugs.

Although passive targeting of nanoparticulates has been proven to localize anti-cancer drugs around cancerous tissues, active targeting strategy employing ligand–receptor specificity were additionally employed to strengthen tumor-specificity of nanoparticulated anti-cancer drugs. Thus, many tumor-specific moieties were immobilized on the nanoparticulated anti-cancer drugs such as many growth factors, whose receptor expressions predominantly appear in tumor-related tissues. Among those, an epidermal

* Corresponding author at: Department of Biomaterials Engineering, School of Bioscience and Bioengineering, Kangwon National University, Chuncheon 200-701, Republic of Korea. Tel.: +82 33 250 6563; fax: +82 33 253 6560.
E-mail address: hsyoo@kangwon.ac.kr (H.S. Yoo).

0378-5173/$ – see front matter © 2009 Elsevier B.V. All rights reserved.
doi:10.1016/j.ijpharm.2009.08.039

growth factor receptor (EGFR) is one of the widely employed targeting moieties because the over-expression is observed in various tumors including lung, breast, ovarian and colorectal carcinoma (Hermanson, 2008).

Therefore, many researchers employed many ligands to delivery nanoparticulated anti-cancer drugs to EGFR-overexpressing tumors (Hu et al., 2008; Park et al., 2006; Ishida et al., 2001). Dual ligands composed of folate and monoclonal antibody against epidermal growth factor receptor (EGFR) was covalently attached to liposomal carriers composed of 1,2-distearoyl-sn-glycerophosphoethanolamine (DSPE) (Jabr-Milane et al., 2008). Combinatorial anti-cancer effects were observed when folate and the antibody were simultaneously immobilized on the nano-carrier. However, compared to attaching small molecules including folate, attaching macromolecules on nanoparticulated drugs was not effective for active targeting because the ligands frequently experience in vivo degradation and inactivation.

In this study, doxorubicin nano-aggregates were prepared for specific-targeting of EGFR-expressing tumor cells. Doxorubicin was chemically conjugated to bi-functional PEG and an EGF peptide was subsequently conjugated to the doxorubicin conjugate to prepare doxorubicin nano-aggregates in aqueous solution. In vitro release profiles and in vitro anti-cancer effects of the nano-aggregates were evaluated to determine active targeting effects of the doxorubicin nano-aggregates.

2. Materials and methods

2.1. Materials

Doxorubicin (DOX) was kindly donated from Korea United Pharm Inc. (Seoul, Korea). Bi-functional poly(ethylene glycol) [NH_2-PEG-COOH] (MW = 3400) and methoxy poly(ethylene glycol) [mPEG-SPA] (MW = 2000) were purchased from Nektar Therapeutics (San Carlos, CA). An EGF fragment (EGFfr) with an amino acid sequence of NH_2-MYIEALDKYAC-COOH was synthesized by Peptron Inc. (Daejon, Korea). Recombinant human epidermal growth factor (rhEGF) was kindly donated from Daewoong (Seoul, Korea). N-succinimidyl 3-(2-pyridyldithio)propionate (SPDP) was obtained from Pierce (Rockford, IL). 1,3-Dicyclohexyl-carbodiimide (DCC), N-hydroxysuccinimide (NHS), and triethylamine (TEA) were purchased from Sigma–Aldrich (St. Louis, MO). Human lung carcinoma cell line (A549) and Chinese Hamster Ovary cell line (CHO) were obtained from Korea Cell Line Bank (Seoul, Korea). RPMI1640 medium, fetal bovine serum (FBS), and LIVE/DEAD® viability/cytotoxicity kit were purchased from Invitrogen corp. (Carlsbad, CA). 3-(4,5-Dimethylthiazol-2yl)-2,5-diphenyltetrazolium bromide (MTT) was obtained from Trevigen Inc. (Gaithersburg, MD). All other chemicals were of analytical grades.

2.2. Preparation of EGFfr-PEG-DOX conjugate

A terminal amine group of NH_2-PEG-COOH was conjugated to a sulfhydryl group of a terminal Cys residue in EGFfr and then a terminal carboxyl group of the conjugate was subsequently conjugated to an amine group of doxorubicin. 26 mg of NH_2-PEG-COOH and 7 mg of SPDP was completely dissolved in 5 ml of dimethylsulfoxide (DMSO) and the reaction was performed at 37 °C for 12 h. The reaction was terminated by adding 25 ml of deionized water (DW) and the reaction mixture was heated to 37 °C for additional 12 h to reduce the volume of the reaction mixture. The sulfhydryl-reactive PEG in a DMSO/water mixture was reacted with 10 mg of EGFfr for 12 h. The resultant EGFfr-PEG-COOH solution was dialyzed against DW three times using a dialysis membrane (Spectrapor6, MW cut-off = 3500) and freeze-dried to prepare EGFfr-PEG-COOH. 35 mg of the EGFfr-PEG-COOH was activated with 4.6 mg of DCC and 4.3 mg of NHS in 6 ml of DMSO. The amine-reactive PEG conjugate was reacted with 4.4 mg of doxorubicin at 37 °C for 12 h in the presence of 0.9 mg of TEA (EGFfr-PEG-COOH/doxorubicin/TEA molar ratio = 1:1:1.2). The resultant solution was dialyzed against DW three times to remove unreacted doxorubicin and other chemicals (Spectrapor6, MW cutoff = 3500). Conjugation process was monitored by reversed phase chromatography using a C_{18} column employing a mixture of acetonitrile and water (3:7) as an isocratic mobile phase. A single peak of the conjugate was detected by a UV detector (254 nm). Conjugation amounts of doxorubicin and EGFfr to PEG were quantitatively determined by elemental analysis and ^{1}H NMR spectroscopy in DMSO-d_6 (EA1110-FISONS, Bruker DPX 400 MHz). Conjugation amounts of doxorubicin to PEG were determined by measuring an absorbance of a conjugate-dissolved solution at 480 nm.

2.3. Preparation of mPEG-DOX conjugate

PEG conjugates without EGFfr was prepared by conjugating amine-reactive mPEG (mPEG-SPA) to amine groups of doxorubicin as described in the literature with a minor modification (Kataoka et al., 2000). Briefly, 76.2 mg of mPEG-SPA in 15 ml of DMSO was reacted with 17 mg of doxorubicin in 4 ml of DMSO at 40 °C for 12 h in the presence of 3.6 mg of TEA (mPEG-SPA/doxorubicin/TEA molar ratio = 1:1:1.2). Unreacted doxorubicin and other chemicals were removed by an extensive dialysis with an aforementioned method and freeze-dried to prepare doxorubicin conjugated mPEG (mPEG-DOX).

2.4. Fabrication and characterization of doxorubicin nano-aggregates (NA)

In order to prepare doxorubicin NA with EGFfr (EGFfr NA), 10% blend ratio (w/w) of EGFfr-PEG-DOX was employed with respect to total polymer weight of NA. Briefly, a mixture of mPEG-DOX (9 mg) and EGFfr-PEG-DOX (1 mg) in 2 ml of acetone was added very slowly to 5 ml of DW with doxorubicin and TEA (DOX in EGFfr-PEG-DOX:doxorubicin:TEA molar ratio = 1:2:2.4). The acetone was evaporated and then the resultant solution was dialyzed against DW three times to remove unentrapped doxorubicin and free conjugates. The solution was concentrated using Centricon® ultracel YM-3 (Millipore, MW cutoff = 3000). For preparation of doxorubicin NA without EGFfr (mPEG NA), 10 mg of mPEG-DOX was employed instead of a mixture composed of mPEG-DOX and EGFfr-PEG-DOX. Loading amount of free doxorubicin in doxorubicin NAs was determined by measuring an absorbance of un-encapsulated free doxorubicin at 480 nm. The size and morphology of doxorubicin NAs was measured by dynamic laser scattering (DLS) and transmission electron microscopy (TEM). For a comparative study for TEM and DLS with free doxorubicin loaded NAs, doxorubicin NA without free doxorubicin was prepared by directly dispersing the conjugates in organic phase into aqueous phase with gently stirring (DOX in EGFfr-PEG-DOX/TEA molar ratio = 1:1.2).

2.5. Cellular uptake of doxorubicin NAs

In order to evaluate selective cellular uptake of doxorubicin in EGFfr NA via EGF receptor-mediated endocytosis, A549 cells and CHO cell were seeded on a 12-well plate at a cell density of 1×10^5 cells/ml in RPMI1640 supplemented with 10% FBS. After 24 h, cells were pre-incubated in serum free RPMI1640 with or without 1 μM of rhEGF for 2 h prior to addition of EGFfr NA or mPEG NA solutions (final concentration of doxorubicin equivalent = 40 μM). After 1.5 h incubation, the cells were visualized by confocal laser scanning microscopy (CLSM) (LSM510, Carl Zeiss,

Germany) with an excitation wavelength at 488 nm and an emission wavelength at 510 nm.

2.6. Cytotoxicity assay

In order to determine cytotoxic activities of doxorubicin NAs, MTT-based cytotoxicity assay was performed with a minor modification (Komoriya et al., 1984). Briefly, A549 cells and CHO cells were seeded on 96-well plate at cell density of 5×10^3 cells/ml in RPMI1640 supplemented with 10% FBS and were pre-incubated in serum free RPMI1640 with or without 1 μM of rhEGF. After 2 h, the incubated cells were exposed to EGFfr NA, mPEG NA, and free doxorubicin and further incubated for 3 h, followed by additional 21 h of incubation in RPMI 1640 with 10% FBS. Ten microliters of MTT solution (5 mg/ml) was added to each well and then the cells were incubated for 4 h. After removing the culture media, DMSO/glycine buffer was added to dissolve formazan crystal and percentage of cell viability was determined using at 570 nm (Bio-tek/EL800PC).

2.7. Live/dead assay

Live/dead cell assay was performed to visually establish a discrepancy of cytotoxicity induced free doxorubicin, EGFfr NA or mPEG NA. A549 cells and CHO cells were seeded on a 12-well plate at a cell density of 1×10^5 cells/ml and were pre-incubated in serum-free media with or without 1 μM of rhEGF for 2 h and then were exposed to free doxorubicin, EGFfr NA or mPEG NA with 30 μM of doxorubicin equivalents for 6 h. Cells were washed three times and were stained with in a live/dead assay kit using two solutions composed of calcein AM and ethidium homodimer-1. After 20 min, the solutions were discarded and the stained cells were washed three times with PBS and were fixed using 2.5% formaldehyde for 30 min. Confocal microscopy was performed to visualize live and dead cells stained with calcein AM and ethidium homodimer-1, respectively, at a band pass filter (500–525 nm) and a long pass filter (560 nm). Percentages of dead cells were image-analyzed by counting the number of cells stained in red with respect to that of total cells (ImagePro, Cybernetics Inc.).

2.8. Animal study

Female athymic nude mice were subcutaneously injected with 1×10^8 cell/animal of A549 cell. When the inoculated tumor volume reached approximately 100 mm^3, doxorubicin, EGFfr NA, and mPEG NA dissolved in 100 μl of PBS were injected through tail veins of the animals through 29G needles. The amount of administered doxorubicin equivalents was kept at 5 mg/kg. In order to measure the tumor size, a major axis (a) and a minor axis (b) of the tumor were measured by a caliper. A tumor volume was determined by calculating as (tumor volume = $(a \times b^2)/2$).

2.9. Statistical analysis

All results were expressed in means ± standard deviation. Statistical significance was determined by one way analysis of variance (ANOVA) followed by a Shaffer's post hoc test for multiple comparisons. $p < 0.05$ was considered statistically significant.

3. Results and discussion

Fig. 1 shows synthetic routes of EGFfr-PEG-DOX and mPEG-DOX. In order to confirm successful conjugation amounts of EGFfr to PEG, ^{1}H NMR spectroscopy was employed and an amide bond between EGFfr and PEG was detected at 8.3 ppm (Suppl. 1). For more quantitative analysis of EGFfr conjugation to the conjugate, an elemental analysis was performed for EGFfr-PEG-DOX and mPEG-DOX as

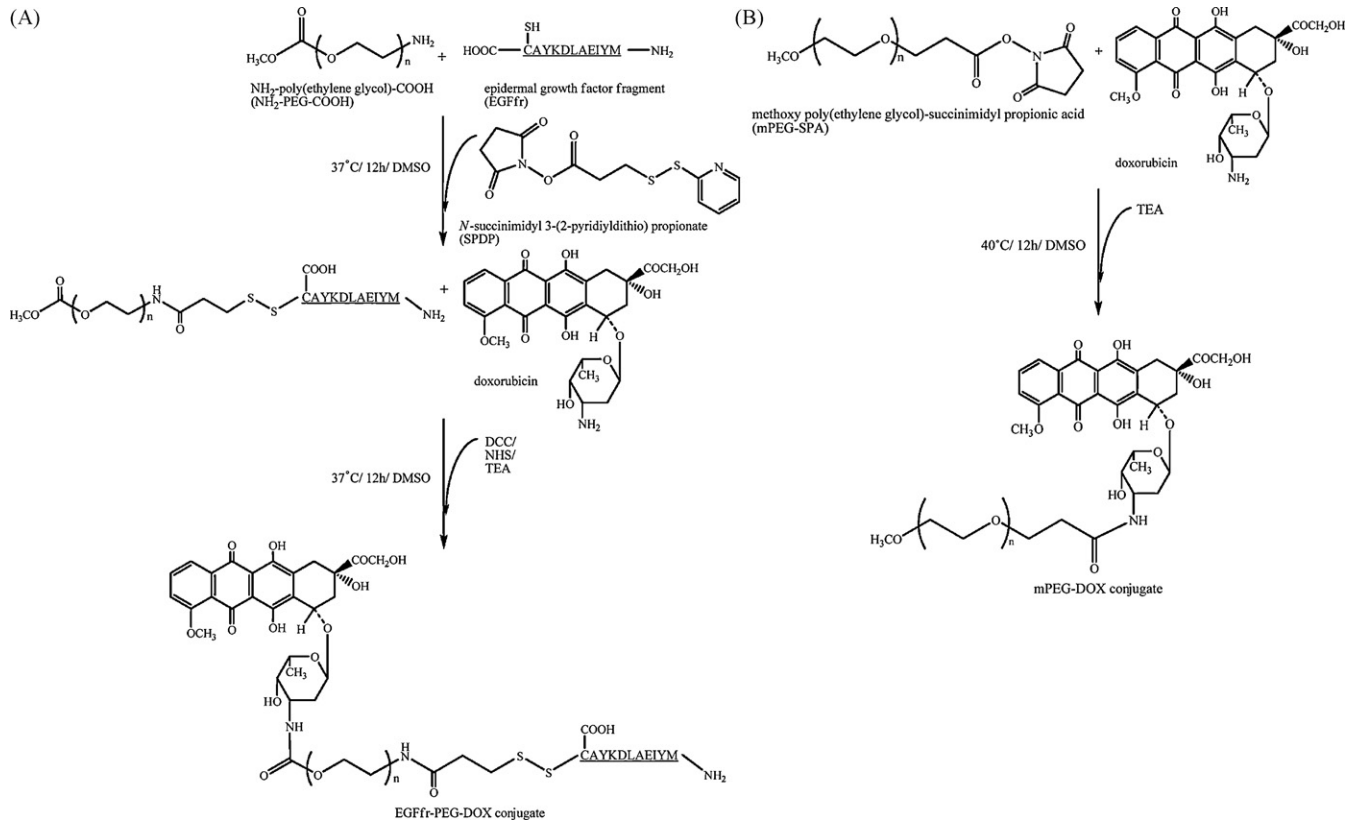

Fig. 1. Synthesis of (A) EGFfr-PEG-DOX conjugate and (B) mPEG-DOX conjugate.

Table 1
Elemental analysis of EGFfr-PEG-DOX conjugate and mPEG-DOX conjugate.

Atom	EGFfr-PEG-DOX conjugate (w/w, %)	mPEG-DOX conjugate (w/w, %)
Nitrogen	5	1
Carbon	53	53
Hydrogen	8	9
Sulfur	2	N/D[a]

[a] Not detected.

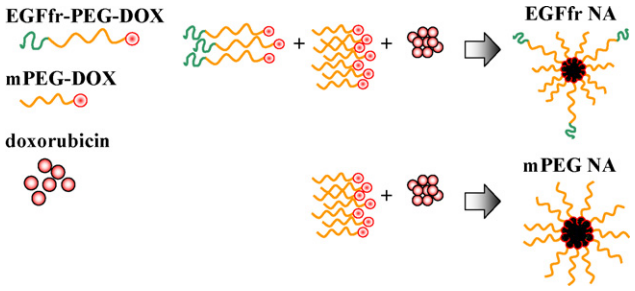

Fig. 2. Schematic diagram of preparing nano-aggregates with EGRfr for tumor targeting.

shown in Table 1. Conjugation amount of EGFfr to the conjugate could be precisely determined by measuring relative contents of elemental sulfur in the conjugate because EGFfr and PEG were coupled by a disulfide linkage. Table 1 indicated elemental sulfur was predominantly detected in EGFfr-PEG-DOX conjugates while no sulfur was detected in mPEG-DOX per se. The amount of conjugated EGFfr in EGFfr-PEG-DOX was 2% (w/w) based on the amount of elemental sulfur, whose value was calculated based on the amount of elemental sulfur with respect to that of elemental carbon. Conjugation of doxorubicin to the conjugate was determined by measuring absorbance of the conjugates at 480 nm. The amount of conjugated doxorubicin to EGFfr-PEG-DOX and mPEG-DOX were 6.6% and 20% (w/w), respectively. However, it should be noticed that the doxorubicin conjugates do not show the same cytotoxicity as free doxorubicin with the same absorbance at 480 nm as previously shown (Freshney, 1994).

Fig. 2 schematically describes a preparation method of doxorubicin NAs with EGF moieties on the surface. For EGF receptor targeting, a fragment composed of CAYKDLAEIYM (11 amino acids) was employed because the EGF fragment was capable of adhering to EGF receptors with a comparable efficiency (*ca.* 80%) according the previous study (Lutsenko et al., 2002). Conjugation of EGF fragment is advantageous over conventional conjugation of intact EGF in several points. Undesirable side-reactions could be minimized such as a disulfide bond exchange reaction because intact EGF contains 6 Cys in the amino acid sequence, which could subsequently decrease EGF binding efficiencies of the conjugate. However, in the current study, only a sulfhydryl group of the terminal Cys in the entire amino acid sequence was employed for conjugation to PEG chains. Thus, the coupling reaction of the peptide to the PEG did not prevent EGFfr-PEG-DOX from binding to EGF receptors because a sequence between 20th and 31st amino acids was considered to be critical in EGF receptor binding (Maeda et al., 2000).

The doxorubicin conjugates and TEA treated doxorubicin spontaneously form nano-scaled aggregates in aqueous solution by hydrophobic interactions between doxorubicin moieties in the conjugate and hydrophobized free doxorubicin (Brannon-Peppas and Blanchette, 2004). TEA played an important role in transforming water-soluble doxorubicin into a water-insoluble form by scavenging chloride ion of a doxorubicin salt form. Several studies previously showed that free doxorubicin loading within nanoparticulated drug carriers was further enhanced when free doxorubicin was encapsulated with the nano-carriers in presence of TEA (Oda et al., 2005). Thus, the core of the NAs is composed of doxorubicin moieties and free doxorubicin while EGFfr was displayed on the outer layer of the nano-aggregates. It should be noted that 10% blend ratios (w/w) of EGFfr-PEG-DOX to all conjugates were employed for preparation of EGFfr NAs according to the literatures (Freshney, 1994).

Doxorubicin NAs were characterized by dynamic light scattering and TEM as shown in Table 2 and Fig. 3. The amounts of encapsulated free doxorubicin within mPEG-DOX NA and EGFfr-PEG-DOX NA were 22.2% (w/w) and 14.4% (w/w), respectively, which were determined by measuring an absorbance of unencapsulated doxorubicin after formulating doxorubicin NAs. Hydrophobized doxorubicin has been shown to efficiently interact with the doxorubicin moieties of the conjugates because of non-covalent π–π coupling of anthracycline rings in doxorubicin moieties and native doxorubicin (Freshney, 1994; Oda et al., 2005). Thus, loading amounts of doxorubicin are totally dependent on an amount of available doxorubicin moieties of the doxorubicin conjugates. Considering the number of doxorubicin moieties per one conjugate were almost the same between mPEG-DOX and EGFfr-PEG-DOX, the amounts of encapsulated doxorubicin in the NAs was considered to be same. However, compared to mPEG-DOX NA, EGFfr-PEG-DOX NA apparently showed lower encapsulation of doxorubicin within NA. This can be explained with molecular weight differences between mPEG-DOX and EGFfr-PEG-DOX. Firstly, a length of the PEG segment in mPEG-DOX is shorter than that of EGFfr-PEG-DOX by 1.4 kDa as described in Materials. EGFfr conjugation to PEG-DOX additionally increased a molecular weight of the conjugate by 1.3 kDa. Thus, the molecular weight difference of 2.7 kDa decreased relative amount of doxorubicin moieties in the same amount of the conjugates when EGFfr-PEG-DOX was employed for physical encapsulation of doxorubicin. Thus, amounts of physically entrapped doxorubicin in EGFfr NAs became lower than those in mPEG NAs. This also suggested that total amounts of doxorubicin equivalents composed of doxorubicin and conjugated doxorubicin in mPEG-DOX NAs were higher than those in EGFfr-PEG-DOX NAs as shown in Table 2. Average diameters of NAs showed similar size by dynamic light scattering (DLS), which ranged from *ca.* 180 nm to *ca.* 280 nm, suggesting doxorubicin NAs were successfully formulated with encapsulating free doxorubicin. TEM also characterized shapes and sizes of doxorubicin NAs where

Table 2
Doxorubicin nano-aggregates (NA) with or without free doxorubicin.

	Amount of free doxorubicin in NA[a] (w/w, %)	Total amount of doxorubicin in NA[b] (free doxorubicin + conjugated DOX, w/w (%))	Average diameter[c] (nm)
mPEG-DOX NA without free doxorubicin	0	16	187.3 ± 2.3
EGFfr-PEG-DOX NA without free doxorubicin	0	6.6	280.5 ± 13.8
mPEG-DOX NA with free doxorubicin (mPEG NA)	22.2	44.9	256.7 ± 11.2
EGFfr-PEG-DOX NA with free doxorubicin (EGFfr NA)	14.4	34.4	228 ± 8.7

[a] Calculated based on the unencapsulated doxorubicin within doxorubicin NAs.
[b] Doxorubicin moieties in the conjugate were detected at 480 nm.
[c] Dynamic light scattering determined the average diameters and standard deviations of NAs.

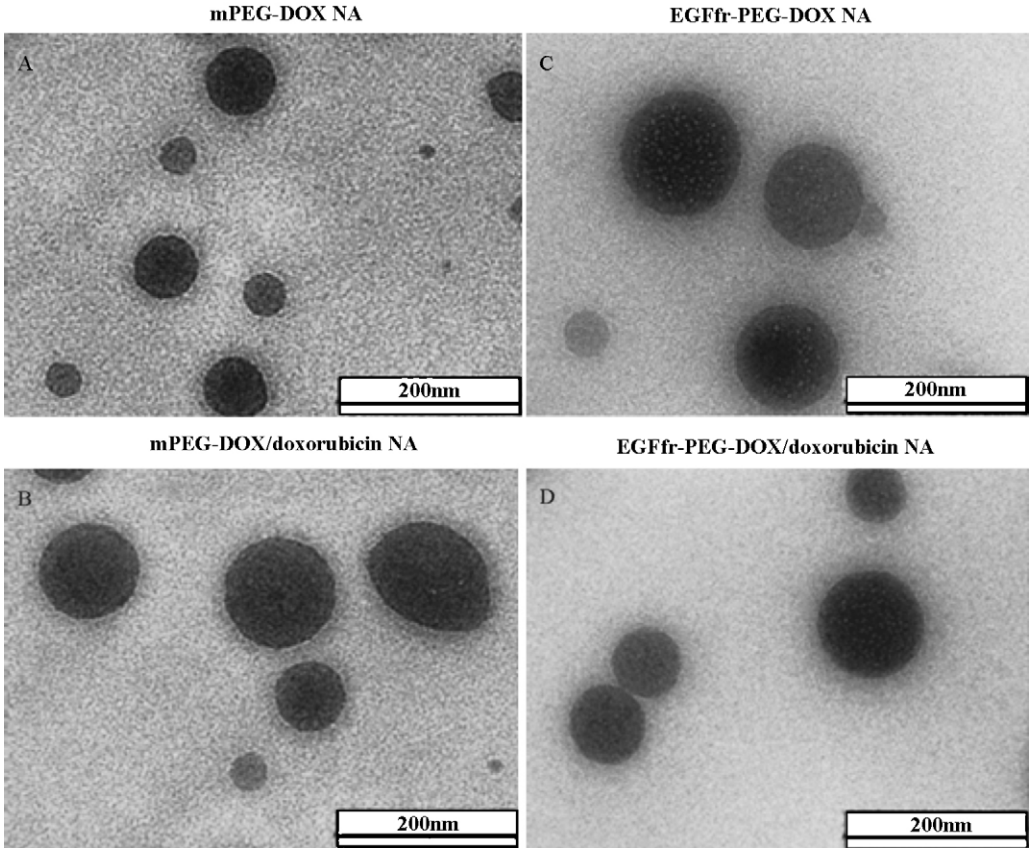

Fig. 3. Transmission electron microscopy (TEM) of NA. (A) mPEG-DOX NA was composed of mPEG-DOX conjugates, (B) mPEG-DOX/doxorubicin NA was formed with mPEG-DOX conjugates and doxorubicin, (C) EGFfr-PEG-DOX NA was composed of EGFfr-PEG-DOX conjugates, and (D) EGFfr-PEG-DOX/doxorubicin NA was formed with EGFfr-PEG-DOX conjugates and doxorubicin.

size distributions ranged from *ca.* 80 nm to *ca.* 130 nm (Fig. 3). Encapsulation of free doxorubicin within NAs did not significantly change shapes and sizes of NAs. The size difference between DLS and TEM can be attributed to difference in NAs status. For TEM examination, NAs were completely dried and PEG chains were consequently collapsed. However, in DLS, NAs in aqueous environ-

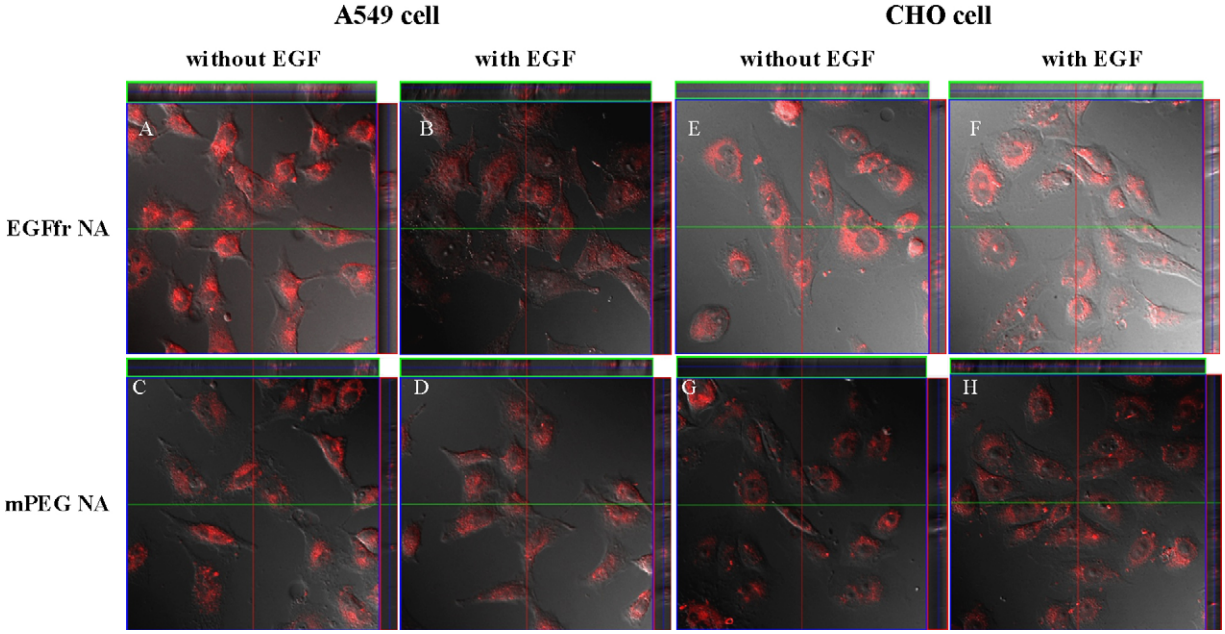

Fig. 4. Confocal laser scanning microscopy of (A–D) A549 cell and (E–H) CHO cell. All cells were pre-incubated in serum free media for 2 h before exposure to DOX for 1.5 h. (A, B, E, and F) Cells were treated EGFfr NA and (C, D, G, and H) cells were treated mPEG NA. (A, C, E, and G) Cells were pre-incubated without EGF and (B, D, F, and H) cells were pre-incubated with EGF (concentration of EGF = 1 μM).

ments showed larger sizes because the PEG chains in NAs were fully extended. Therefore, we concluded that encapsulation of doxorubicin within doxorubicin NAs did not change size and morphology of the NAs. Thus, we employed doxorubicin NAs composed of EGFfr-PEG-DOX [EGFfr NA] and mPEG-DOX [mPEG NA] for the current studies.

A cellular uptake of nanoparticulated drugs is an important parameter to measure in vitro efficiency of nano-sized colloidal drug carriers with targeting moieties because drug efficacy is frequently dependent on a degree of cellular uptake. Thus, targeting effects of doxorubicin NAs were compared in an EGFR-overexpressing cell line (A549) and a cell line showing minimal levels of EGFR expressions (CHO) as shown in Fig. 4. A large amount of EGFfr NA was endocytosed by A549 cell compared to mPEG NA in the absence of EGF in solution (Fig. 4A and C). However, when the cell was pre-incubated with 1 μM of rhEGF, no difference in cellular uptakes was found between EGFfr NA and mPEG NA. This result clearly demonstrated that the surface-exposed EGFfr significantly facilitates cellular uptakes of doxorubicin NAs compared to unmodified NA because no significant morphological difference was found between EGFfr NA and mPEG NA according to Fig. 3 and Table 2. In Fig. 4B and D, however, most EGF receptors were pre-blocked by 2 h incubation with EGF, suggesting that EGFfr on the NAs could not enhanced endocytosis of doxorubicin NAs. In contrast to the results with A549 cells, CHO cells incubated with both NAs did not show any noticeable differences in endocytic uptakes of doxorubicin NAs (Fig. 4E–H). Thus, regardless of pre-incubation of EGF, EGFfr could not enhance uptakes of doxorubicin NAs in A549 cells. Again, this result clearly demonstrated that facilitated endocytosis of EGFfr NA was attributed to a ligand–receptor interaction between EGFfr and EGFR because CHO cells does not overexpress EGFR. In addition, it is very significant that the cellular localization of doxorubicin NAs was different from free doxorubicin as shown in previous studies (Qiu and Bae, 2006; Sahu et al., 2008). Free doxorubicin diffuses into cells by a simple diffusion and directly access to nuclear regions while NAs remains in lysosomal and endosomal compartments. Free doxorubicin within a cytosol is easily pumped out by a specialized pump at cytosolic membranes for a multi-drug resistance (MDR), which is considered to be a major cause of anti-cancer drug resistance (Saul et al., 2006; Son et al., 2003). However, endocytosed NAs cannot be easily pumped out because they are encapsulated in the cellular compartments, subsequently increasing an anti-cancer efficacy of doxorubicin. Conjugation of EGFfr to NAs is considered to further facilitate endocytic process of NAs because EGFR is normally endocytosed upon complexation with EGF at cellular membranes (Lutsenko et al., 2002; Verdière et al., 1994). Furthermore, an EGFR-EGF complex in a cytosol is destined to a nuclear region because the complex binds to a promoter region of ELK, NF-κB and c-Fos genes to promote cellular proliferation (Yoo et al., 1999, 2000). Thus, endocytosed doxorubicin NAs with EGFfr are also expected to be localized within nuclear regions where doxorubicin should be localized for anti-cancer effects. Thus, unlike other targeting moieties for tumor cells such as folate, EGFR targeting is more attractive because localization of doxorubicin NA is occurred both in tumors cells and in nucleus of tumor cells.

In vitro anti-cancer effect of doxorubicin NAs was determined by a MTT-based cytotoxicity assay as shown in Fig. 5. Compared to doxorubicin NAs, doxorubicin showed higher cytotoxicity against tumor cells employed. However, the degree of cytotoxicity was dependent on the presence of EGFR on cell surfaces. EGFfr NA exerted higher cytotoxicity against A549 cells (A) than CHO cells (B) while no difference was found when mPEG NA was administered to both cells with statistical significances ($p < 0.05$). This could be attributed to increased binding efficiency of EGFfr NA toward A549 cells due to a specific interaction between EGFfr and EGFR whose effects were already shown in Fig. 4. However, it was of noticeable that both NAs showed inferior cytotoxicity to doxorubicin in A549 cells and CHO cells. For the cytotoxicity assay, cells were incubated with doxorubicin NAs for 24 h, which was consequently insufficient to measure cytotoxic effects of the NAs against cells. NAs normally follow endocytic pathways to gain an access to nuclear regions while doxorubicin can freely diffuse into the regions. Thus, this requires adequate time for doxorubicin NAs to show cytotoxicity, however, 24 h of incubation with cells was not enough to show cytotoxicity of doxorubicin NAs. Similar cytotoxicity results were observed in other studies employing nanoparticulated doxorubicin where free doxorubicin exerted higher cytotoxicity than doxorubicin nanoparticles when the nanoparticles were incubated with cells for 24–48 h before a MTT-based cytotoxicity assay (Yoo and Park, 2001).

A LIVE/DEAD® cell assay was employed to precisely measure the effects of cytotoxicity of doxorubicin NAs as shown in Fig. 6. In culture media without EGF, EGFfr NA showed superior cytotoxicity against A549 cells to mPEG NA, where cytotoxicity increased

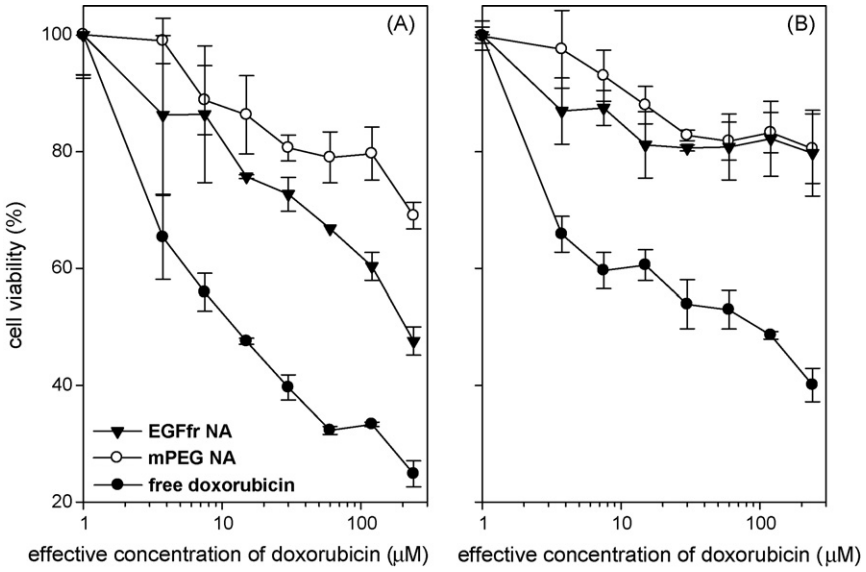

Fig. 5. MTT-based cytotoxicity assay of (A) A549 cell and (B) CHO cell incubated with NAs. All cells were pre-incubated in serum-free media for 2 h and then were exposed to each sample for 3 h, followed by additional 21 h incubation in RPMI1640 with FBS.

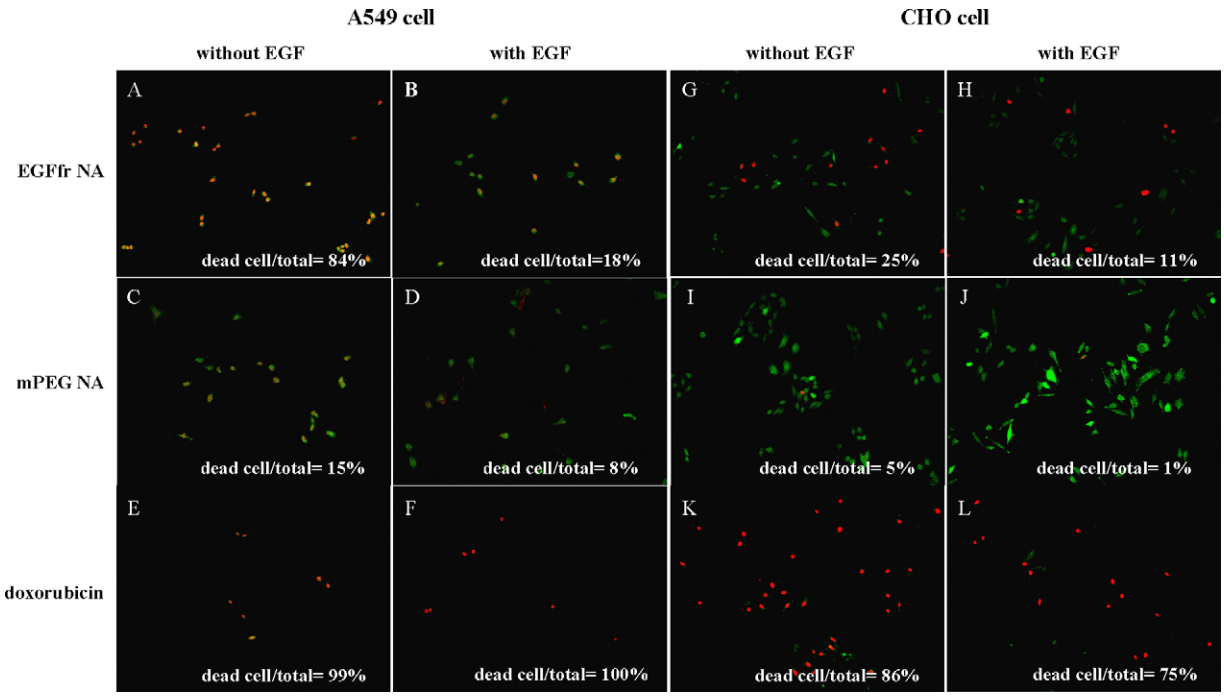

Fig. 6. Live/dead assay of A549 cell and CHO cell incubated with EGFfr NA (A, B, G, and H), mPEG NA (C, D, I, and J), and doxorubicin (E, F, K, and L). All cells were pre-incubated in serum-free media for 2 h before 6h-exposure to each sample. Cells in green and in red indicate live and dead cells, respectively.

by 1.8 folds. It is also encouraging that EGFfr NA showed a comparable cytotoxicity to native doxorubicin (100%) because cells were exposed to doxorubicin NAs only for 6 h. However, mPEG NA showed decrease cytotoxicity as low as 56% in the presence of EGF when IC_{50} values were compared. Endocytosed doxorubicin NA subsequently undergoes endocytic pathways, which is a rate determining step for entry to a nuclear region, while native doxorubicin easily access to a nuclear region by a simple diffusion. This suggests that nanoparticulated doxorubicin is inferior to native doxorubicin in terms of exerting in vitro cytotoxicity for a short period. Other studies employing doxorubicin nanoparticulates also indicated that in vitro cytotoxicity assay did not show superior cytotoxicity to native doxorubicin when nanoparticulated doxorubicin was incubated with cells for a short period (Brekken et al., 2000; Freshney, 1994; Yoo and Park, 2004). In the current study, EGFfr of the doxorubicin NAs was confirmed to further enhance cytotoxicity of doxorubicin NAs by increasing endocytic uptakes of doxorubicin NAs and the degree of cytotoxicity was comparable to that of native doxorubicin. CHO cells with doxorubicin NAs did not show any differences in cytotoxicities (Fig. 5G–J). This is again attributed to minimal expression levels of EGFR in CHO cells. Although EGFfr NA was administered to CHO cells, enhanced uptake by the cell could not occur because of a decreased interaction between EGFR and EGFfr and the same level of cytotoxicity was consequently measured as mPEG NA was administered. This also coincides with the results of Figs. 4 and 5 showing no difference in cytotoxicity and endocytosis was found in CHO cells. Therefore, it is concluded that facilitated cellular uptakes of doxorubicin NAs caused increased cytotoxicity of EGFfr NAs against EGFR-overexpressing cancer cells. However, it should be mentioned that cells were exposed to doxorubicin NAs for 6 h while they were exposed for 3 h in MTT-based cytotoxicity assay. The difference in the exposure time could be attributed to post-incubation time of the MTT assay (21 h) that could allow doxorubicin NAs to exert cytotoxic effects. Thus, in case of the live/dead cell assay, a longer exposure period was required to monitor the differences in cytotoxicity because the post-incubation period was absent.

In order to determine in vivo cytotoxicity of doxorubicin NAs, female athymic nude mouse bearing human lung adenocarcinoma was administered with doxorubicin NAs and their tumor sizes were measured as shown in Fig. 7. Compared to free doxorubicin, EGFfr NA showed higher anti-cancer efficacy after 14 days. During the first week after administration, however, doxorubicin significantly decreased tumor volumes compared to the other groups. This is attributed to fast diffusion of free doxorubicin into cancerous tissues and cells. Unlike doxorubicin NAs that should be endocytosed by cells, doxorubicin directly access to nuclear regions thorough cellular membranes by a simple diffusion. While a simple diffusion supports a fast acting of the anti-cancer agent, free doxorubicin can be easily pumped out by cancer cells. As shown in Fig. 7, the tumor volume of the animals with free doxorubicin slowly recovered to the original status because of MDR effects by cancer cells. However, the administered doxorubicin NAs showed better cytotoxicity

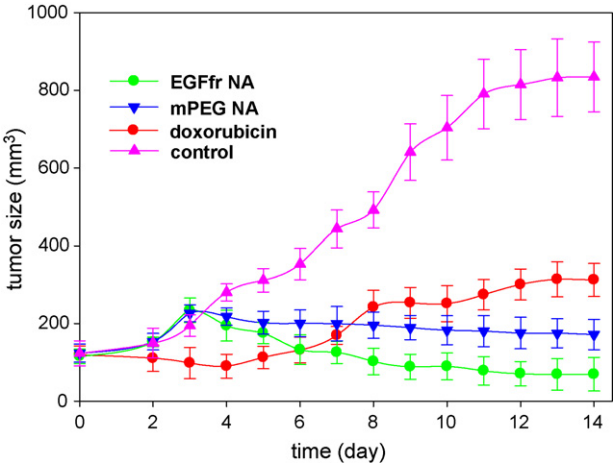

Fig. 7. In vivo anti-cancer effects of doxorubicin NAs. Doxorubicin equivalents (5 mg/kg) were intravenously injected to ICR mouse bearing human lung carcinoma through tail veins.

after the first week. Endocytosed NAs undergo endosomal pathways to enter nuclear regions, which is a time-consuming process compared to free diffusion of native doxorubicin. Thus, it has been previously shown that nanoparticulated drugs showed a sustained anti-cancer effect compared to native anti-cancer drugs as shown in other studies (Brannon-Peppas and Blanchette, 2004; Freshney, 1994; Yoo and Park, 2001).

EGFfr decoration on the NA significantly increased in vivo anti-cancer effects of doxorubicin NAs with a statistical significance ($p < 0.05$, EGFfr NA and mPEG NA). Both EGFfr NA and mPEG NA showed delayed-type anti-cancer effects against human lung carcinoma during the first week of administration compared to free doxorubicin, However, EGFfr NA more efficiently reduced the tumor sizes compared to mPEG NA after the first week. In addition, it should be also noticed that EGFR targeting of anti-cancer drugs has several disadvantages compared to other targeting moieties for active targeting. EGF itself significantly promotes proliferation of cancer cells because EGF strongly binds to EGFR overexpressing cancer cells and initiates signal transduction process. However, in the current study, EGFfr-decorated doxorubicin NAs did not enhance proliferation of the targeted cancer cells while several studies previously indicated that decoration drug carriers with EGF increased proliferation of cancer cells and reversed effects of anti-cancer drug (Ciardiello and Tortora, 2001; Rebeca et al., 2009; Hoeling et al., 2009). This often leaded to a failure of anti-cancer therapy employing EGF-EGFR receptor strategy because tumor tissue well proliferated compared to native anti-cancer drugs. However, in order to determine why EGFfr showed minimal effects on cellular proliferation of EGFR-overexpressing cancer cells, further studies would be required to confirm binding mechanisms of EGFfr to EGFR compared to native EGF.

4. Conclusion

Decorating doxorubicin NA with EGFfr increased endocytic uptakes by A549 cells. Furthermore, the EGFfr NA showed better cytotoxicity compared to mPEG NA, however, pre-blocking of EGFR of A549 cells significantly reduced the cytotoxicity of EGFfr NA. In vivo studies revealed that EGFfr NAs effectively suppressed tumor growth and regression after 2 weeks compared to native doxorubicin and unmodified doxorubicin NAs. Thus, EGFfr NA is expected to be a potent anti-cancer drug carrier against EGFR-overexpressing cancer cells.

Acknowledgements

This study was supported by a grant from the National R&D Program for Cancer Control, Ministry for Health, Welfare and Family affairs, Republic of Korea (grant #: 0620280) and Kangwon National University (grant #: C105744-01-01).

Appendix A. Supplementary data

Supplementary data associated with this article can be found, in the online version, at doi:10.1016/j.ijpharm.2009.08.039.

References

Allen, T.M., 2002. Ligand-targeted therapeutics in anticancer therapy. Nat. Rev. Cancer 2, 750–763.
Blessing, T., Kursa, M., Holzhauser, R., Kircheis, R., Wagner, E., 2001. Different strategies for formation of pegylated EGF-conjugated PEI/DNA complexes for targeted gene delivery. Bioconjugate Chem. 12, 529–537.
Brannon-Peppas, L., Blanchette, J., 2004. Nanoparticle and targeted systems for cancer therapy. Adv. Drug Deliv. Rev. 56, 1649–1659.
Brekken, R.A., Overholser, J.P., Stastny, V.A., Waltenberger, J., Minna, J.D., Thorpe, P.E., 2000. Selective inhibition of vascular endothelial growth factor (VEGF) receptor 2 (KDR/Flk-1) activity by a monoclonal anti-VEGF antibody blocks tumor growth in mice. AACR, 5117–5124.
Byrne, J.D., Betancourt, T., Brannon-Peppas, L., 2008. Active targeting schemes for nanoparticle systems in cancer therapeutics. Adv. Drug Deliv. Rev. 60, 1615–1626.
Ciardiello, F., Tortora, G., 2001. A novel approach in the treatment of cancer: targeting the epidermal growth factor receptor. Clin. Cancer Res. 7, 2958–2970.
Freshney, R.I., 1994. Culture of Animal Cells, 5th ed. Wiley-Liss Inc, pp. 359–373.
Hermanson, G.T., 2008. Bioconjugate Techniques, 2nd ed. Elsevier, pp. 171–172.
Hoeling, T., Siperstein, A.E., Clark, O.H., Duh, Q.Y., 2009. Epidermal growth factor enhances proliferation, migration, and invasion of follicular and papillary thyroid cancer in vitro and in vivo. J. Clin. Endocrinol. Metab. 79, 401–408.
Hu, F., Wu, X., Du, Y., You, J., Yuan, H., 2008. Cellular uptake and cytotoxicity of shell crosslinked stearic acid-grafted chitosan oligosaccharide micelles encapsulating doxorubicin. Eur. J. Pharm. Biopharm. 69, 117–125.
Ishida, O., Maruyama, K., Tanahashi, H., Iwatsuru, M., Sasaki, K., Eriguchi, M., Yanagie, H., 2001. Liposomes bearing polyethyleneglycol-coupled transferrin with intracellular targeting property to the solid tumors in vivo. Pharm. Res. 18, 1042–1048.
Jabr-Milane, L.S., Vlerken, L.E., Yadav, S., Amili, M.M., 2008. Multi-functional nanocarriers to overcome tumor drug resistance. Cancer Treat. Rev. 34, 592–602.
Kataoka, K., Matsumoto, T., Yokoyama, M., Okano, T., Sakurai, Y., Fukushima, S., Okamoto, K., Kwon, G., 2000. Doxorubicin-loaded poly(ethylene glycol)–poly(β-benzyl-L-aspartate) copolymer micelles: their pharmaceutical characteristics and biological significance. J. Control. Rel. 64, 143–153.
Komoriya, A., Hortsch, M., Meyers, C., Smith, M., Kanety, H., Schlessinger, J., 1984. Biologically active synthetic fragments of epidermal growth factor: localization of a major receptor-binding region. Proc. Natl. Acad. Sci. U.S.A. 81, 1351–1355.
Lutsenko, S.V., Feldman, N.B., Severin, S.E., 2002. Cytotoxic and antitumor activities of doxorubicin conjugates with the epidermal growth factor and its receptor-binding fragment. J. Drug Target. 10, 567–571.
Maeda, H., Wu, J., Sawa, T., Matsumura, Y., Hori, K., 2000. Tumor vascular permeability and the EPR effect in macromolecular therapeutics: a review. J. Control. Rel. 65, 271–284.
Oda, K., Matsuoka, Y., Funahashi, A., Kitano, H., 2005. A comprehensive pathway map of epidermal growth factor receptor signaling. Mol. Syst. Biol., 11–17.
Park, J.H., Kwon, S., Lee, M., Chung, H., Kim, J., Kim, Y., Park, R., Kim, I., Seo, S.B., Kwon, I.C., Jeong, S.Y., 2006. Self-assembled nanoparticles based on glycol chitosan bearing hydrophobic moieties as carriers for doxorubicin: in vivo biodistribution and anti-tumor activity. Biomaterials 27, 119–126.
Qiu, L.Y., Bae, Y.H., 2006. Polymer architecture and drug delivery. Pharm. Res. 23, 1–30.
Rebeca, A.M., Elaine, V.M., Margaret, R.K., Karl, T.K., Carmen, J.M., Alan, R.S., Angeline, S.A., 2009. EGFR pathway polymorphisms and bladder cancer susceptibility and prognosis. Carcinogenesis 30, 1155–1160.
Sahu, A., Bora, U., Kasoju, N., Goswami, P., 2008. Synthesis of novel biodegradable and self-assembling methoxy poly(ethylene glycol)—palmitate nanocarrier for curcumin delivery to cancer cells. Acta Biomater. 4, 1752–1761.
Saul, J.M., Annapragada, A.V., Bellamkonda, R.V., 2006. A dual-ligand approach for enhancing targeting selectivity of therapeutic nanocarriers. J. Control. Rel. 114, 277–287.
Son, Y.J., Jang, J.S., Cho, Y.W., Chung, H., Park, R.W., Kwon, I.C., Kim, I., Park, J.Y., Seo, S.B., Park, C.R., Jeong, S.Y., 2003. Biodistribution and anti-tumor efficacy of doxorubicin loaded glycol-chitosan nanoaggregates by EPR effect. J. Control. Rel. 91, 135–145.
Verdière, A.C., Dubernet, C., Nemati, F., Poupon, M.F., Puisieux, F., Couvreur, P., 1994. Uptake of doxorubicin from loaded nanoparticles in multidrug-resistant leukemic murine cells. Cancer Chemother. Pharmacol. 33, 504–508.
Yoo, H.S., Park, T.G., 2001. Biodegradable polymeric micelles composed of doxorubicin conjugated PLGA–PEG block copolymer. J. Control. Rel. 70, 63–70.
Yoo, H.S., Park, T.G., 2004. Folate receptor targeted biodegradable polymeric doxorubicin micelles. J. Control. Rel. 96, 273–283.
Yoo, H.S., Oh, J.E., Lee, K.H., Park, T.G., 1999. Biodegradable nanoparticles containing doxorubicin-PLGA conjugate for sustained release. Pharm. Res. 16, 1114–1118.
Yoo, H.S., Lee, K.H., Oh, J.E., Park, T.G., 2000. In vitro and in vivo anti-tumor activities of nanoparticles based on doxorubicin-PLGA conjugates. J. Control. Rel. 68, 419–431.